PHOTONICS Research

Passively spatiotemporal gain-modulation-induced stable pulsing operation of a random fiber laser

Jiangming Xu,[1,2,3] Jun Ye,[1] Wei Liu,[1] Jian Wu,[1,2] Hanwei Zhang,[1,2] Jinyong Leng,[1,2] and Pu Zhou[1,2,*]

[1]College of Optoelectronic Science and Engineering, National University of Defense Technology, Changsha 410073, China
[2]Hunan Provincial Collaborative Innovation Center of High Power Fiber Laser, Changsha 410073, China
[3]e-mail: jmxu1988@163.com
*Corresponding author: zhoupu203@163.com

Received 12 July 2017; revised 28 August 2017; accepted 14 September 2017; posted 15 September 2017 (Doc. ID 302271); published 26 October 2017

Unlike a traditional fiber laser with a defined resonant cavity, a random fiber laser (RFL), whose operation is based on distributed feedback and gain via Rayleigh scattering (RS) and stimulated Raman scattering in a long passive fiber, has fundamental scientific challenges in pulsing operation for its remarkable cavity-free feature. For the time being, stable pulsed RFL utilizing a passive method has not been reported. Here, we propose and experimentally realize the passive spatiotemporal gain-modulation-induced stable pulsing operation of counter-pumped RFL. Thanks to the good temporal stability of an employed pumping amplified spontaneous emission source and the superiority of this pulse generation scheme, a stable and regular pulse train can be obtained. Furthermore, the pump hysteresis and bistability phenomena with the generation of high-order Stokes light is presented, and the dynamics of pulsing operation is discussed after the theoretical investigation of the counter-pumped RFL. This work extends our comprehension of temporal property of RFL and paves an effective novel avenue for the exploration of pulsed RFL with structural simplicity, low cost, and stable output.

OCIS codes: (140.3490) Lasers, distributed-feedback; (290.5870) Scattering, Rayleigh; (290.5910) Scattering, stimulated Raman.

https://doi.org/10.1364/PRJ.5.000598

1. INTRODUCTION

A random fiber laser (RFL), whose operation is based on the extremely weak Rayleigh scattering (RS) provided random distributed feedback (RDFB) and Raman gain in a section of passive fiber, has attracted increasing attention in the past decades for its special features of cavity-free, mode-free, and structural simplicity, and for its application potential in telecommunication and distributed sensing [1–4]. The recent developments of RFL mainly focus on the power scaling [5–7], polarization operating [8,9], wavelength tuning [10,11], linewidth narrowing [12–14], spectral coverage extending [15,16], application for frequency doubling [17], mid-infrared light source pumping [18,19], and so on [4].

Generally speaking, most of the previous presented RFLs operate in a continuous-wave state with stable output. As we know, pulsed fiber lasers (mode-locked or *Q*-switched ones) have a wide range of appealing applications and can be achieved via an active or passive method depending on whether or not a modulator is included in the cavity [20–24]. Although mode locking and taming of random lasers formed by nanoscale particles have been realized via mode-selective pumping [25] and active control of the spatial pump profile [26], a pulsing operation state of Raman fiber laser based on a piece of relevantly long fiber with definite resonant cavity has been reported [27,28]; pulsing operation of RFLs based on hundreds of meters and even kilometers of passive fiber has fundamental scientific challenges for their remarkable cavity-free features [22,23]. Additionally, mode-locking technologies, as important routes to obtain a pulsed laser for traditional fiber lasers [20,21], are generally not applicable to mode-free RFLs [29]. Recently, pulsed RFLs have been demonstrated via active modulation methods such as internal modulation utilizing electro-optical modulator [22], *Q*-switching with the aid of an acousto-optic modulator [23,24], polarization modulation employing polarization switch, and arbitrary waveform generator [30]. Simultaneously, passively methods, for instance, *Q*-switching assisted by stimulated Brillouin scattering (SBS) [31,32] and saturable absorption of monolayer grapheme [29,33], are also important schemes for the demonstration of pulsed RFLs. Furthermore, Zhang *et al.* [34] in our group

reported the passive self-oscillation with obvious amplitude instability and continuous-wave pedestal in high-order RFL, which was attributed to the depletion of the pump. It is worth noting that obtaining a stable pulse from an RFL based on a passive method is difficult for the stochastic nature of RDFB and SBS [35].

In this paper, we propose and realize a stable pulsed RFL via passive spatiotemporal gain modulation. The RFL in a half-opened cavity is counterpumped by a powerful and temporal stable amplified spontaneous emission (ASE) source. The measurements in temporal and frequency domains can prove the good stability of an output pulse train. Furthermore, the theoretical simulations can fit the experimental results well and present the spatiotemporal distributions of pump and Stokes light in the long passive fiber. Based on this, the dynamics of pulsing operation are discussed. Moreover, pump hysteresis and bistability can be observed for output pulse, power, and spectrum with the overcoming of the threshold of second-order Stokes light. To the best of our knowledge, this is the first demonstration of stable pulsing operation of RFL by a passive modulation method.

2. EXPERIMENTAL SETUP AND RESULTS

The experimental setup of the counterpumped RFL is plotted in Fig. 1. A fiber coupler with a coupling ratio of 50:50 at 1080 nm is utilized as the fiber loop mirror (FLM) to supply optical feedback by splicing the output ports together. The measured FLM reflection coefficient for the first- and second-order Stokes light is about 90% and 50%, respectively. Additionally, a piece of 3 km long passive fiber (G.652, 8.2 μm core diameter, and 0.14 numerical aperture) is employed to offer RDFB and Raman gain for the random lasing. Then, a half-opened cavity [36] can be achieved, whose optical feedback is provided both by the highly reflective point feedback (PFB) from FLM and the weakly random distributed RS in the passive fiber. The pump source we utilized is a broadband ASE light centered at 1079.2 nm with an FWHM linewidth of about 17 nm. The pump light is injected into the passive fiber via the first port of fiber circulator. And the random laser light is coupled out from the cavity via the third port of the fiber circulator.

Figure 2 illustrates the output power and spectral characteristics of this counterpumped RFL. Below the pump threshold of Stokes light generation (3.5 W pump power entering the passive fiber), only transmitted pump light can be observed in the output light from the third port of a fiber circulator. With the increment of pump power from 3.5 to 6.51 W, unstable random lasing can be measured with the aid of an optical spectrum analyzer (OSA, 0.02 nm optical resolution), InGaAs photodetector (5 GHz bandwidth, rise time <70 ps) and digital phosphor oscilloscope (1 GHz bandwidth). As shown in Fig. 2(b), several high-order Stokes light and lots of spikes in the output spectrum can be observed with 5.36 W pump light injected, which is typical for the multicascaded RS-SBS generation [2,37]. The corresponding temporal characteristic of output Stokes light at 5.36 W pump level is depicted in Fig. 3(a). A regular pulse train and irregular giant pulse coexist in the output signals, which agree well with the reported on–off and multistate intermittencies of RFL near the threshold in Ref. [38]. With the enhancement of pump power to 6.51 W, the high-order Stokes light vanishes, and the output spectrum becomes smooth. Furthermore, a regular pulse train can be obtained at this power level, as plotted in Fig. 3(b). The period of the output pulse is 37.42 μs, which is about 1.27 times higher than the round-trip time $2nL/c$ (n is the refraction index of fiber, L is the length of the cavity, and c is the speed of light in vacuum) in the passive fiber. In contrast with the round-trip time, the increment of pulse period value may be partly influenced by the multiple-scattering-induced effective optical path enhancement in the long fiber [2,36]. Furthermore, as the Stokes light can experience optical gain and loss simultaneously in the fiber, the increasing of pulse period value also may be caused by the increment of effective length of the long fiber, which is defined by $L_{\text{eff}} = [1 - \exp(-\alpha L)]/\alpha$ (α is determined by gain and loss jointly) [39]. Additionally, a more complete investigation is worth studying. As to the power characteristics, based on the measurements of spectrum and power of output light from the third

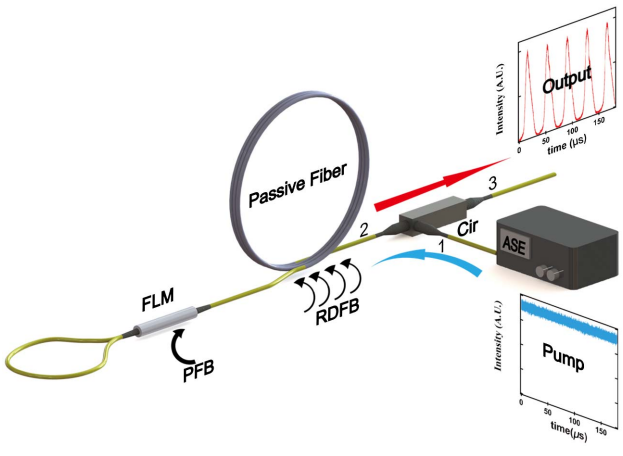

Fig. 1. Experimental setup of the counterpumped RFL. Cir, circulator.

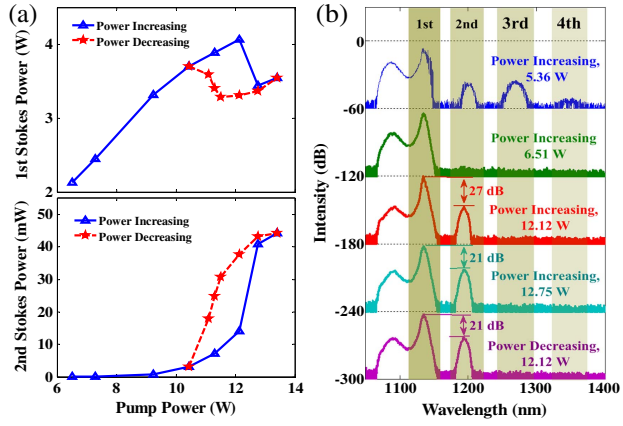

Fig. 2. Power and spectrum characteristics of the counterpumped RFL. (a) Corresponding power of first- and second-order Stokes light as functions of pump power. (b) Output spectra at different pump levels.

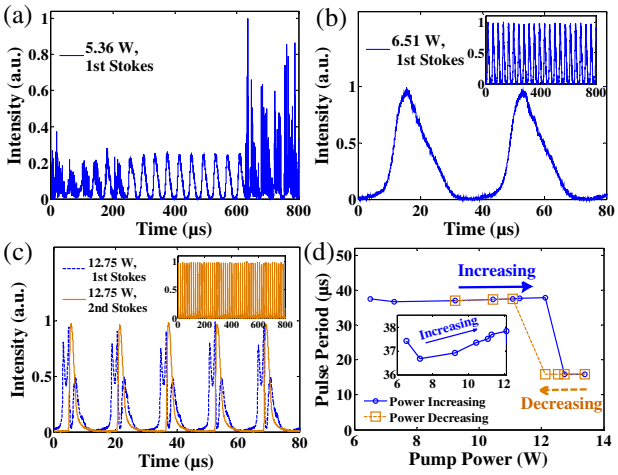

Fig. 3. Temporal characteristics of output pulse. Signals of output first-order Stokes light at (a) 5.36 and (b) 6.51 W pump powers. (c) Shapes of output first- and second-order Stokes light at 12.75 W pump level. (d) Evolution of period as function of pump power.

port of fiber circulator with the aid of OSA and power meter, the average power of output first-order Stokes light is estimated to be 2.13 W by numerically spectral integrating. The corresponding energy of the pulse envelope is evaluated to be about 79.7 μJ. The dynamics of the pulsing operation will be explained in the following simulation section. With the scaling of pump power from 6.51 to 12.12 W, tiny changing of pulse period can be measured, as shown in Fig. 3(d). This may be attributed to the alteration of optical gain in the fiber with the enhancement of pump level, as the output pulse is associated with the pump depletion and Raman gain in the passive fiber. At pump power of 12.12 W, the estimated average power of output first-order Stokes light is 4.07 W. Furthermore, the optical peak corresponding to the second-order Stokes light can be observed with intensity 27.14 dB lower than the optical peak of first-order Stokes light at this pump level.

The threshold of second-order Stokes light of this RFL is about 12.75 W. At this pump level, dramatic increasing of average power of second-order Stokes light and decreasing of average power of first-order Stokes light can be measured, as presented in Fig. 2(a). Additionally, the difference of intensity of first- and second-order Stokes light decreases to 20.89 dB. Simultaneously, the pulse period of the first- and second-order Stokes light both decrease to 15.89 μs, which is similar to the transmit time (nL/c, 14.72 μs) in the passive fiber. The changing of pulse period may also be induced by the alteration of optical gain and loss in the fiber and agrees well with previously reported results in Ref. [34]. Unlikely, the lasing tendency of first- and second-order Stokes light from this RFL cannot be concluded simply as anti-phase motion as described in the previous manuscript. Despite the sharing of the same pulse period, the pulse shapes of first- and second-order Stokes light are not completely identical, as displayed in the Fig. 3(c). The corresponding energies of pulse envelopes of first- and second-order Stokes light are calculated to be about 54.66 and 0.65 μJ, respectively.

Worthy of mention here is that the pulse period always jumps at a relatively high pump power level (12.75 W, threshold of second-order Stokes light) in the power scaling process, and the transformation of output power and spectrum can be simultaneously measured. In the pump power decreasing process, the operation state could be maintained to a relatively low pump level (11.09 W) until the pulse period drastically increases. This phenomenon is known as pump hysteresis and bistability [40,41], which may be induced by the refractivity modulation of the optical intensity or the gain saturation in the long passive fiber of this pulsed RFL. The pump hysteresis and bistability characteristics indicate that the operation state of this laser can be influenced by not only the pump level but also by the initial state. Further dynamical investigation is ongoing.

The radio-frequency (RF) characteristics and long-time operation of output pulses from this counterpumped RFL are also measured. Figures 4(a) and 4(c) plot the corresponding RF spectra of the first- and second-order Stokes light measured at the fundamental repetition frequency with pump power of 6.51 and 12.75 W (threshold of first- and second-order Stokes light). The RF traces have contrasts of about 60 and 62 dB against the noise floor, respectively, which indicate good stability of the output pulse and may be benefited from the good stability feature of employed pumping ASE source [42]. Additionally, the amplitudes are only 39.2 and 46.2 dB for the RFL pumped by traditional fiber laser in linear cavity structure, which is similar with that presented in Fig. 1(a) of Ref. [36]. Figures 4(b) and 4(d) show the RF spectra of long-time operation (100 s) of this RFL from 0 to 1 MHz with 6.51 and 12.75 W pump power. The RF spectra keep stable in the long time measurements. The measurements of RF characteristics prove that stable pulsation can be obtained from this counterpumped RFL.

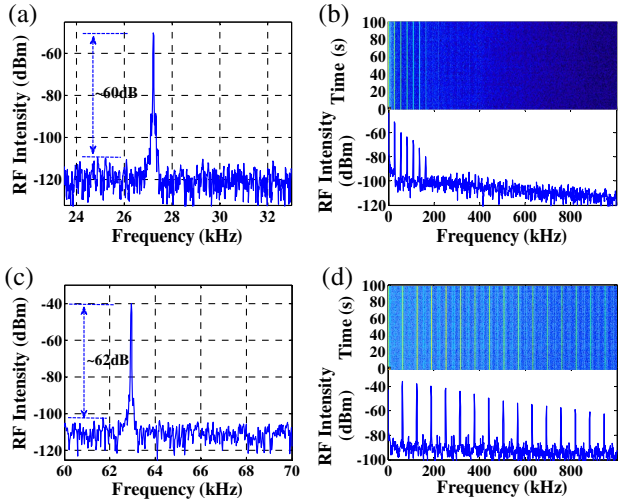

Fig. 4. RF spectra of (a) first-order Stokes light and (c) second-order Stokes light around fundamental repetition frequency with a resolution of 20 Hz. Long-time recording of RF spectra of (b) first-order Stokes light and (d) second-order Stokes light in the range of 0–1 MHz with a resolution of 200 Hz and length of 100 s.

3. SIMULATION OF PULSING OPERATION DYNAMICS

The pulsing operation of this counterpumped RFL can be theoretically investigated by a set of temporal-spatial-coupled cascaded Raman equations with the considering of distributed Rayleigh backward scattering [6,34]:

$$\frac{dP_0^{\pm}}{dz} \pm \frac{1}{v_{g0}}\frac{dP_0^{\pm}}{dt} = \mp\frac{\lambda_1}{\lambda_0}g_{R1}(P_1^+ + P_1^- + 4h\nu_1\Delta\nu_1 B_1)P_0^{\pm} \mp \alpha_0 P_0^{\pm} \pm \varepsilon_0 P_0^{\mp}, \quad (1)$$

$$\frac{dP_1^{\pm}}{dz} \pm \frac{1}{v_{g1}}\frac{dP_0^{\pm}}{dt} = \pm g_{R1}(P_0^+ + P_0^-)(P_1^{\pm} + 2h\nu_1\Delta\nu_1 B_1 \pm \varepsilon_0 P_1^{\mp}) \mp \frac{\lambda_2}{\lambda_1}g_{R2}(P_2^+ + P_2^- + 4h\nu_2\Delta\nu_2 B_2)P_1^{\pm} \mp \alpha_1 P_1^{\pm}, \quad (2)$$

$$\frac{dP_2^{\pm}}{dz} \pm \frac{1}{v_{g2}}\frac{dP_2^{\pm}}{dt} = \mp g_{R2}(P_1^+ + P_1^-)(P_2^{\pm} + 2h\nu_2\Delta\nu_2 B_2) \mp \alpha_2 P_2^{\pm}, \quad (3)$$

$$B_j = 1 + \frac{1}{\exp\left[\frac{h(\nu_j - \nu_{j-1})}{k_B T}\right] - 1} \qquad (j = 1, 2), \quad (4)$$

where the subscript 0, 1, and 2 stands for the pump light, the first-order Stokes light, and the second-order Stokes light, respectively; superscripts+and−represent the forward and backward propagating waves, correspondingly; $P(z, t)$ denotes the power in different time and position; ν_g is the group velocity in the fiber; g_R, α, and ε is the Raman gain coefficient, signal loss and Rayleigh backscattering coefficient, respectively. h is Planck constant; υ is the wave frequency; $\Delta\upsilon$ is the bandwidth of Stokes light. The parameter B represents the population of the photon that introduces the noise from spontaneous Raman scattering.

The boundary conditions can be described as $P_{0,1,2}^+(0, t) = R_{L0,1,2}P_{0,1,2}^-(0, t)$, $P_0^-(L, t) = P_{\text{in}}T_{R0} + R_{R0}P_0^+(L, t)$, $P_{1,2}^-(L, t) = R_{R1,2}P_{1,2}^+(L, t)$, $P_{\text{out}0,1,2}(t) = T_{R0,1,2}P_{0,1,2}^+(L, t)$, where $R_{L0,1,2}$ and $R_{R0,1,2}$ are the corresponding reflectivities at the left and right end, P_{in} stands for the input pump power, and $T_{R0,1,2}$ are the transmissivities of fiber circulator. The values of parameters set in the numerical simulation are listed in Table 1.

Equations (1)–(4) can be numerically solved by discretizing the variables of z and t with the FDTD method. The calculated output power as a function of time at 6.51 W pump power (threshold of first-order Stokes light) is depicted in Fig. 5(a). When $t = 0$, the pump light is turned on and launched into the RFL via the fiber circulator. It takes about 28 μs for the first-order Stokes light coming back to the fiber circulator, which is almost consistent with the round-trip time in the 3 km passive fiber. Just at the established moment, the Stokes light exhibits pulsing operation, and 190 μs later (about six times the round-trip time) the output Stokes light evolves to a regular pulse shape. The peak power of calculated output pulse is about 7.25 W after stable pulse can be obtained. The pulse periods at different pump level (lower than the threshold of second-order Stokes light) are also simulated and plotted in Fig. 5(b). The evolutions of pulse can approximately fit with the experimental data. Generally speaking, the presented model and parameters can be employed to investigate the pulsing operation dynamics of this counterpumped RFL preliminarily.

Table 1. Parameters for the Numerical Calculations

Parameter	Value	Unit
$\lambda_0, \lambda_1, \lambda_2$	1.0792, 1.134, 1.195	10^{-6} m
g_{R1}, g_{R2}	6.3, 6.0	10^{-4} m^{-1} W^{-1}
a_0, a_1, a_2	2.7, 2.2, 1.8	10^{-4} m^{-1}
$\varepsilon_0, \varepsilon_1, \varepsilon_2$	6.5, 6, 5.5	10^{-7} m^{-1}
$\Delta\nu_1, \Delta\nu_2$	0.55, 1.00	10^{12} Hz
T	298	K
R_{L0}, R_{L1}, R_{L2}	0.99, 0.9, 0.5	
R_{R0}, R_{R1}, R_{R2}	2.1×10^{-5}	
T_{R0}, T_{R1}, T_{R2}	0.95, 0.89, 0.82	

To explore the dynamics of the pulsing operation of this counterpumped RFL, the spatial-temporal distributions of pump and Stokes light are calculated and presented in Fig. 6. In this counterpumped RFL, we can imagine the following processes. The output of Stokes light need sufficient Raman gain, which is provided by the pump light distributed in the half-opened cavity. When the pump source with enough power level is on, the pump light, which experiences a round trip in the passive fiber and exports from the third port of fiber circulator, would be depleted because most of its energy will transform to the first-order Stokes light. Then, the pump power distributed in the half-opened cavity at a certain moment cannot provide sufficient Raman gain for the Stokes light, and the RFL could be off. When the RFL is off, the pump light distributed in the cavity would not be depleted and can offer enough Raman gain for Stokes light. Then, a pulse of Stokes light is formed. About six times of round-trip time after turning of the pump source, a kinetic balance between the pump power and Stokes power distributed in the cavity can be achieved and stable spatial-temporal modulation of pump can be generated, as presented in Figs. 6(a) and 6(b). Then, stable pulsing operation can be obtained. In summary, the stable pulsing operation of this counterpumped RFL is caused by the passive spatial-temporal-modulation of pump-light induced self-modulation of Raman gain in the laser despite employing of a continuous-wave pump source.

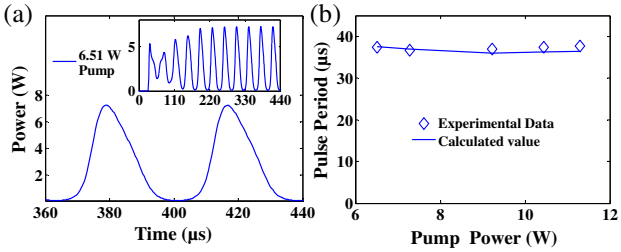

Fig. 5. Calculated (a) output pulse and (b) pulsation period.

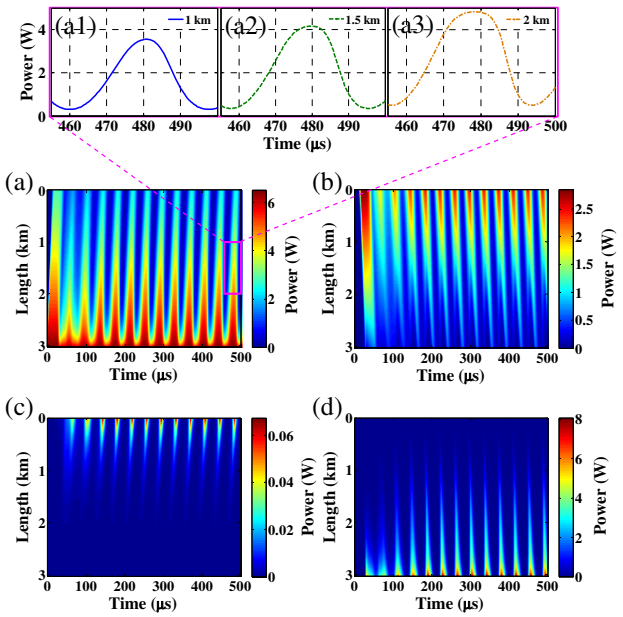

Fig. 6. Spatiotemporal distributions of pump light and Stokes light at threshold of first-order Stokes light. Insertion graphs of (a) present the temporal evolution of backward pump power at three different locations. (a) Backward pump power. (b) Forward pump power. (c) Backward Stokes power. (d) Forward Stokes power.

It should be noted that the generation of pulsed second-order Stokes light pumped by pulsed first-order Stokes light and the pump hysteresis and bistability characteristic cannot be simulated presently with this simple model without the consideration of dispersion, optical-intensity-induced refractivity modulation and interaction length of transmitted pulse. This is our next goal of theoretical investigation.

4. SUMMARY

In conclusion, we propose and realize a stable pulsed RFL via passively spatiotemporal gain modulation. The RFL in a half-opened cavity is counterpumped by a powerful and temporal stable ASE source. At 6.51 W pump level, stable pulse can be obtained with a period of 37.42 μs. The corresponding energy of the pulse envelope is 79.7 μJ. Furthermore, the RF trace at the fundamental repetition frequency has a contrast of as high as 60 dB against the noise floor, which indicates the good stability of the output pulse train. The theoretical simulation fits the experimental result well and presents the spatiotemporal distributions of forward and backward pump light and Stokes light in the long passive fiber. Based on this, we can conclude that the pulsing operation is caused by the passively spatiotemporal modulation of pump light induced self-modulation of Raman gain in the passive fiber despite of the employing of a continuous-wave pump source. Additionally, pump hysteresis and bistability can be observed with the overcoming of threshold of second-order Stokes light. Further pulse energy scaling and dynamical simulations of pump hysteresis and bistability are ongoing. The investigations can extend the comprehension of temporal property of RFL and provide an effective novel avenue for the exploration of pulsed RFL with structural simplicity, low cost, and stable output.

Funding. National Natural Science Foundation of China (NSFC) (61322505, 61635005); Hunan Provincial Innovation Foundation for Postgraduate Student (CX2017B030).

Acknowledgment. We are particularly grateful to Zhiyuan Dou, Ke Yin, and Tong Liu for their elicited discussions.

REFERENCES

1. D. S. Wiersma, "The physics and applications of random lasers," Nat. Phys. **4**, 359–367 (2008).
2. S. K. Turitsyn, S. A. Babin, A. E. El-Taher, P. Harper, D. V. Churkin, S. I. Kablukov, J. D. Ania-Castañón, V. Karalekas, and E. V. Podivilov, "Random distributed feedback fibre laser," Nat. Photonics **4**, 231–235 (2010).
3. W. Zhang, Y. Song, X. Zeng, R. Ma, Z. Yang, and Y. Rao, "Temperature-controlled mode selection of Er-doped random fiber laser with disordered Bragg gratings," Photon. Res. **4**, 102–105 (2016).
4. X. Du, H. Zhang, H. Xiao, P. Ma, X. Wang, P. Zhou, and Z. Liu, "High-power random distributed feedback fiber laser: from science to application," Ann. Der Phys. **528**, 649–662 (2016).
5. Z. Wang, H. Wu, M. Fan, L. Zhang, Y. Rao, W. Zhang, and X. Jia, "High power random fiber laser with short cavity length: theoretical and experimental investigations," IEEE J. Sel. Top. Quantum Electron. **21**, 0900506 (2015).
6. X. Du, H. Zhang, P. Ma, H. Xiao, X. Wang, P. Zhou, and Z. Liu, "Kilowatt-level fiber amplifier with spectral broadening-free property, seeded by a random fiber laser," Opt. Lett. **40**, 5311–5314 (2015).
7. J. Xu, L. Huang, M. Jiang, J. Ye, P. Ma, J. Leng, J. Wu, H. Zhang, and P. Zhou, "Near-diffraction-limited linearly polarized narrow-linewidth random fiber laser with record kilowatt output," Photon. Res. **5**, 350–354 (2017).
8. S. A. Babin, E. A. Zlobina, S. I. Kablukov, and E. V. Podivilov, "High-order random Raman lasing in a PM fiber with ultimate efficiency and narrow bandwidth," Sci. Rep. **6**, 22625 (2016).
9. J. Xu, Z. Lou, J. Ye, J. Wu, J. Leng, H. Xiao, H. Zhang, and P. Zhou, "Incoherently pumped high-power linearly-polarized single-mode random fiber laser: experimental investigations and theoretical prospects," Opt. Express **25**, 5609–5617 (2017).
10. S. A. Babin, A. E. El-Taher, P. Harper, E. V. Podivilov, and S. K. Turitsyn, "Tunable random fiber laser," Phys. Rev. A **84**, 021805 (2011).
11. L. Zhang, H. Jiang, X. Yang, W. Pan, S. Cui, and Y. Feng, "Nearly-octave wavelength tuning of a continuous wave fiber laser," Sci. Rep. **7**, 42611 (2017).
12. M. Pang, X. Bao, and L. Chen, "Observation of narrow linewidth spikes in the coherent Brillouin random fiber laser," Opt. Lett. **38**, 1866–1868 (2013).
13. S. Sugavanam, N. Tarasov, X. Shu, and D. V. Churkin, "Narrow-band generation in random distributed feedback fiber laser," Opt. Express **21**, 16466–16472 (2013).
14. T. Zhu, F. Chen, S. Huang, and X. Bao, "An ultra-narrow linewidth fiber laser based on Rayleigh backscattering in a tapered optical fiber," Laser Phys. Lett. **10**, 055110 (2013).
15. I. A. Lobach, S. I. Kablukov, M. I. Skvortsov, E. V. Podivilov, M. A. Melkumov, S. A. Babin, and E. M. Dianov, "Narrowband random lasing in a Bismuth-doped active fiber," Sci. Rep. **6**, 30083 (2016).
16. X. Jin, Z. Lou, H. Zhang, J. Xu, P. Zhou, and Z. Liu, "Random distributed feedback fiber laser at 2.1 μm," Opt. Lett. **41**, 4923–4926 (2016).
17. E. I. Dontsova, S. I. Kablukov, I. D. Vatnik, and S. A. Babin, "Frequency doubling of Raman fiber lasers with random distributed feedback," Opt. Lett. **41**, 1439–1442 (2016).
18. H. Zhang, P. Zhou, X. Wang, X. Du, H. Xiao, and X. Xu, "Hundred-Watt level high power random distributed feedback Raman fiber laser

at 1150 nm and its application in mid-infrared laser generation," Opt. Express **23**, 17138–17144 (2015).
19. Y. Shang, M. Shen, P. Wang, X. Li, and X. Xu, "Amplified random fiber laser-pumped mid-infrared optical parametric oscillator," Chin. Opt. Lett. **14**, 121901 (2016).
20. E. P. Ippen, "Principles of passive mode locking," Appl. Phys. B **58**, 159–170 (1994).
21. H. A. Haus, "Mode-locking of lasers," IEEE J. Sel. Top. Quantum Electron. **6**, 1173–1185 (2000).
22. M. Bravo, M. Fernandez-Vallejo, and M. Lopez-Amo, "Internal modulation of a random fiber laser," Opt. Lett. **38**, 1542–1544 (2013).
23. A. G. Kuznetsov, E. V. Podivilov, and S. A. Babin, "Actively Q-switched Raman fiber laser," Laser Phys. Lett. **12**, 035102 (2015).
24. J. Xu, J. Ye, H. Xiao, J. Leng, J. Wu, H. Zhang, and P. Zhou, "Narrow-linewidth Q-switched random distributed feedback fiber laser," Opt. Express **24**, 19203–19210 (2016).
25. M. Leonetti, C. Conti, and C. Lopez, "The mode-locking transition of random lasers," Nat. Photonics **5**, 615–617 (2011).
26. N. Bachelard, J. Andreasen, S. Gigan, and P. Sebbah, "Taming random lasers through active spatial control of the pump," Phys. Rev. Lett. **109**, 033903 (2012).
27. B. Burgoyne, N. Godbout, and S. Lacroix, "Transient regime in a n^{th}-order cascaded CW Raman fiber laser," Opt. Express **12**, 1019–1024 (2004).
28. P. Suret, N. Y. Joly, G. Mélin, and S. Randoux, "Self-oscillations in a cascaded Raman laser made with a highly nonlinear photonic crystal fiber," Opt. Express **16**, 11237–11246 (2008).
29. B. Yao, Y. Rao, Z. Wang, Y. Wu, J. Zhou, H. Wu, M. Fan, X. Cao, W. Zhang, Y. Chen, Y. Li, D. Churkin, S. Turitsyn, and C. W. Wong, "Graphene based widely-tunable and singly-polarized pulse generation with random fiber lasers," Sci. Rep. **5**, 18526 (2015).
30. H. Wu, Z. Wang, Q. He, M. Fan, Y. Li, W. Sun, L. Zhang, Y. Li, and Y. Rao, "Polarization-modulated random fiber laser," Laser Phys. Lett. **13**, 055101 (2016).
31. Y. Tang and J. Xu, "A random Q-switched fiber laser," Sci. Rep. **5**, 9338 (2015).
32. S. M. Wang, W. Lin, W. C. Chen, C. Li, C. S. Yang, T. Qiao, and Z. M. Yang, "Low-threshold and multiwavelength Q-switched random erbium-doped fiber laser," Appl. Phys. Express **9**, 032701 (2016).
33. R. Ma, W. Zhang, X. Zeng, Z. Yang, Y. Rao, B. Yao, C. Yu, Y. Wu, and S. Yu, "Quasi mode-locking of coherent feedback random fiber laser," Sci. Rep. **6**, 39703 (2016).
34. H. Zhang, H. Xiao, P. Zhou, X. Wang, and X. Xu, "Random distributed feedback Raman fiber laser with short cavity and its temporal properties," IEEE Photon. Technol. Lett. **26**, 1605–1608 (2014).
35. G. Ravet, A. A. Fotiadi, M. Blondel, and P. Mégret, "Passive Q-switching in all-fibre Raman laser with distributed Rayleigh feedback," Electron. Lett. **40**, 528–529 (2004).
36. D. Churkin, S. Babin, A. E. El-Taher, P. Harper, S. Kablukov, V. Karalekas, J. D. Ania-Castañón, E. Podivilov, and S. K. Turitsyn, "Raman fiber lasers with a random distributed feedback based on Rayleigh scattering," Phys. Rev. A **82**, 033828 (2010).
37. K. D. Park, B. Min, P. Kim, N. Park, J. H. Lee, and J. S. Chang, "Dynamics of cascaded Brillouin-Rayleigh scattering in a distributed fiber Raman amplifier," Opt. Lett. **27**, 155–157 (2002).
38. A. V. Lanin, S. V. Sergeyev, D. Nasiev, D. V. Churkin, and S. K. Turitsyn, "On-off and multistate intermittencies in cascaded random distributed feedback fibre laser," in *Conference on Lasers and Electro-Optics-International Quantum Electronics Conference* (Optical Society of America, 2013), paper IG_P_18.
39. S. K. Turitsyn, S. A. Babin, D. V. Churkin, I. D. Vatnik, M. Nikulin, and E. V. Podivilov, "Random distributed feedback fibre lasers," Phys. Rep. **542**, 133–193 (2014).
40. A. K. Komarov and K. P. Komarov, "Multistability and hysteresis phenomena in passive mode-locked lasers," Phys. Rev. E **62**, R7607–R7610 (2000).
41. A. Zavyalov, R. Iliew, O. Eogrov, and F. Lederer, "Hysteresis of dissipative soliton molecules in mode-locked fiber lasers," Opt. Lett. **34**, 3827–3829 (2009).
42. P. Wang and W. A. Clarkson, "High-power, single-mode, linearly polarized, ytterbium-doped fiber superfluorescent source," Opt. Lett. **32**, 2605–2607 (2007).